

**Electronic supplementary materials** *Mendeleev Commun.*, 2022, **32**, 717–719

**New heterocyclic furazano[3,4-*d*][1,2,3]triazine system as a platform for energetic compound engineering**

**Victor P. Zelenov, Igor L. Dalinger, Aleksey A. Anisimov, Kyrill Yu. Suponitsky, Alla N. Pivkina and Aleksei B. Sheremetev**

CONTENTS

Experimental	S2
Enthalpy of formation	S3
Crystal structure refinement and packing analysis for compound <b>1</b>	S3
References	S7
NMR spectra	S8

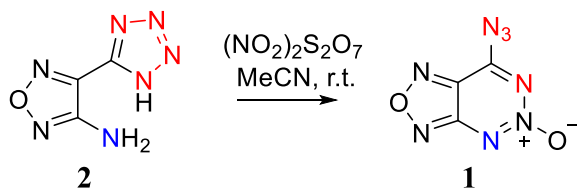
## Experimental

IR spectra were recorded on a BrukerALPHA instrument in KBr pellets.  $^{13}\text{C}$ , and  $^{14}\text{N}$  spectra were acquired on a Bruker AM-300 instrument (75.47 and 21.69 MHz, respectively) in  $\text{CDCl}_3$  or  $\text{DMSO}-d_6$  at 299 K. The chemical shifts of  $^{13}\text{C}$  nucleus were reported relative to TMS, for  $^{14}\text{N}$  – relative to  $\text{MeNO}_2$ , high-field chemical shifts are given with a minus sign. High-resolution mass spectra with electrospray ionization were recorded on a Bruker MicroOTOF II instrument. Elemental analysis was performed on a PerkinElmer 2400 Series II instrument. The reaction progress and purity of the obtained compounds were controlled by TLC on Merck Silicagel 60 F<sub>254</sub> plates. Visualization of spots on TLC plate was accomplished with UV light (254 nm).

**Materials** Most of the reagents and starting materials were purchased from commercial sources and used without additional purification. The starting 3-amino-4-(tetrazol-5-yl)furazan (**2**)<sup>[S1,S2]</sup>, 3-amino-4-(2-hydroxytetrazol-5-yl)furazan (**3**)<sup>[S3,S4]</sup> and nitronium salts<sup>[S5-S7]</sup> were obtained published procedures.

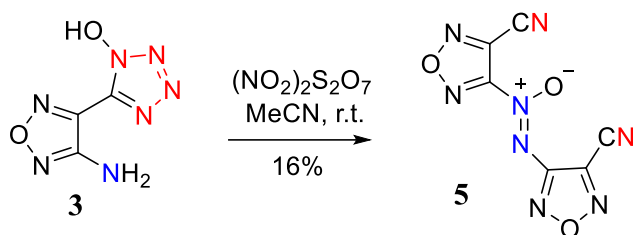
**Caution!** Although we have encountered no difficulties during preparation and handling of these compounds, they are dangerous high explosives. Manipulations must be carried out by using appropriate standard safety precautions.

### 7-Azidofurazano[3,4-*d*][1,2,3]triazine 5-oxide (**1**)



Tetrazole derivative **2** (1.46 g, 9.5 mmol) was added in small portions to a suspension of  $(\text{NO}_2)_2\text{S}_2\text{O}_7$  (7.5 g, 28 mmol) in  $\text{MeCN}$  (60 ml) at 20 °C with stirring under dried conditions. The mixture was stirred at room temperature for 4 h, then diluted with  $\text{CH}_2\text{Cl}_2$  (60 ml), filtered and evaporated. The residue was purified by column chromatography (eluting with 3:1  $\text{CHCl}_3/\text{EtOAc}$ ) to give product **1** (1.17 g, 68%) as colorless crystals.  $R_f = 0.25$  ( $\text{CHCl}_3$  :  $\text{EtOAc}$ , 3:1).  $^{13}\text{C}$  NMR ( $\text{CDCl}_3$ )  $\delta$  131.47, 158.06, 159.47.  $^{14}\text{N}$  NMR ( $\text{CDCl}_3$ )  $\delta$  -47 ( $\Delta\nu_{1/2} = 150$  Hz,  $\text{N} \rightarrow \text{O}$ ), -135 ( $\Delta\nu_{1/2} = 35$  Hz,  $\text{N}_3$ ). IR (KBr): 2246, 2199, 2170, 1617, 1537, 1496, 1461, 1414, 1384, 1365, 1227, 1169, 1055, 1040, 962, 873, 844, 766, 751, 705, 600, 551, 535, 443  $\text{cm}^{-1}$ . MS,  $m/z$ : 180  $[\text{M}]^+$ . HRMS (ESI),  $m/z$  calcd for  $\text{C}_3\text{N}_8\text{O}_2$  181.0220  $[\text{M} + \text{H}]^+$ , found, 181.0217  $[\text{M} + \text{H}]^+$ . Anal. Calcd for  $\text{C}_3\text{N}_8\text{O}_2$  (180.09): C, 20.01; N, 62.22. Found: C, 20.08; N, 62.19.

### 4,4'-Dicyanoazoxyfurazan (**5**)



Under dried conditions compound **3** (1.56 g, 9.2 mmol) was added in small portions with stirring to a suspension of  $(\text{NO}_2)_2\text{S}_2\text{O}_7$  (6.2 g, 23 mmol) in MeCN (70 ml) at  $5^\circ\text{C}$  (in an ice-bath) upon which the mixture thickened and gas release was observed. After the addition was complete, the reaction was stirred for 2 h at  $15\text{--}20^\circ\text{C}$  and then diluted with  $\text{CH}_2\text{Cl}_2$  (70 ml), filtered and evaporated. The residue was purified by column chromatography (eluting with 3:1  $\text{CHCl}_3/\text{EtOAc}$ ,  $R_f = 0.33$ ). Product containing fractions were combined and solvent removed *in vacuo* to give crude product **5** as a bluish solid, which crystallized from  $\text{CHCl}_3/\text{EtOAc}$  as colorless needles; yield: 176 mg (16%); mp  $169\text{--}169.5^\circ\text{C}$ .  $^{13}\text{C}$  NMR ( $\text{CDCl}_3$ )  $\delta$  106.1, 107.0, 130.6, 131.8, 154.8, 159.9;  $^{14}\text{N}$  NMR ( $\text{CDCl}_3$ )  $\delta$   $-69$  ( $\Delta\nu_{1/2} = 250$  Hz,  $\text{N}\rightarrow\text{O}$ ). IR (KBr): 2272, 1563, 1517, 1472, 1448, 1403, 1330, 1226, 1155, 1127, 1034, 937, 891, 775, 612, 582, 550,  $422\text{ cm}^{-1}$ . MS,  $m/z$ : 232  $[\text{M}]^+$ . HRMS (ESI),  $m/z$  calcd for  $\text{C}_6\text{N}_8\text{O}_3$  254.9980  $[\text{M} + \text{Na}]^+$ , found: 254.9986  $[\text{M} + \text{Na}]^+$ . Anal. Calcd for  $\text{C}_6\text{N}_8\text{O}_3$  (232.12): C, 31.05; N, 48.28. Found: C, 31.13; N, 48.24.

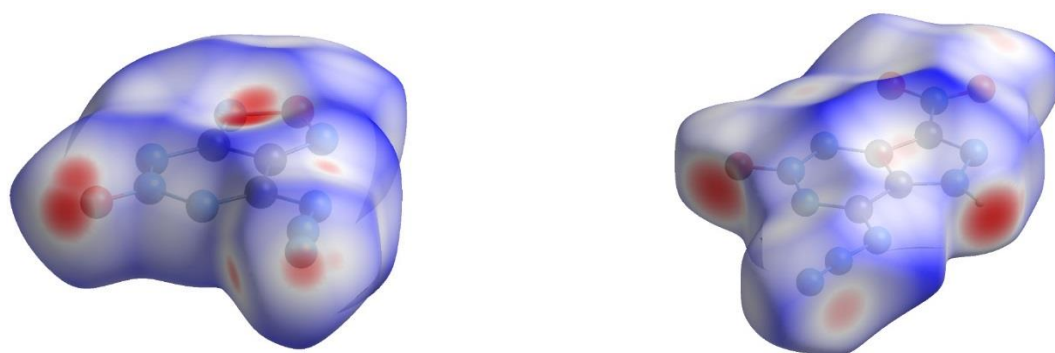
### Enthalpy of formation

The enthalpy of formation in the gas phase for compound **1** was calculated by using the program package Gaussian 03 (G3B3)<sup>[S8]</sup> and converted to the enthalpy of formation in the condensed phase ( $\Delta_f H_{(s)} = \Delta_f H_{(g)} - \Delta H_{\text{subl}}$ ) taking into account the enthalpy of sublimation calculated in accordance with the Trouton rule:  $\Delta H_{\text{subl}} = (188 \cdot T_m(\text{K})/1000)/4.184$ .<sup>[S9]</sup>

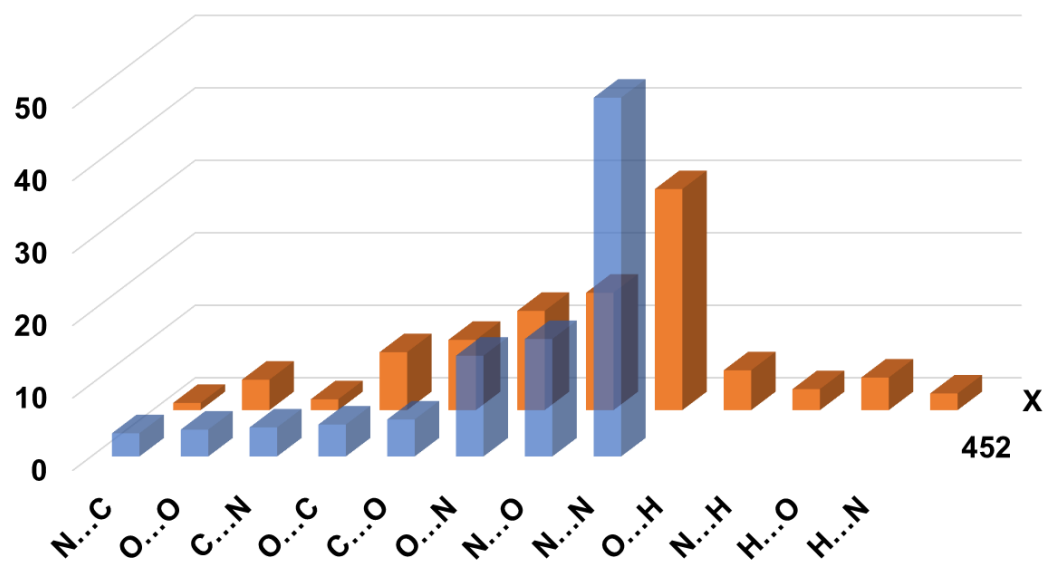
## Crystal structure refinement and packing analysis for compound **1**

It is interesting to compare crystal packing of the present compound **1** with its nitropyrazole analog.<sup>[S11]</sup> We analyzed crystal packing of 452 and X compounds using the Crystal Explorer code.<sup>[S12]</sup> The difference of sensitivity values for compound **1** and **NAPTO** appears to be in line with the analysis of Hirshfeld surfaces<sup>[S13]</sup> and distributions of types of close contacts penetrating these surfaces (see Figures S1 and S2). Indeed, the puck-like shape of Hirshfeld surface observed for **NAPTO** is known to indicate an anisotropic crystal packing (in particular, of layer type) and low sensitivity values for high-energetic solids.<sup>[S14]</sup> At the same time, although the distribution of contacts for compound **1** is characterized by larger positive kurtosis (5.63 vs. 3.72 for **NAPTO**), its standard deviation is also larger than that for **NAPTO** (15.77% vs. 8.48%). Moreover, nearly 50% of close contacts in compound **1** correspond to the N...N type (N...pi interactions) and are distributed rather uniformly over the Hirshfeld surface (Figure S3). In the other words, the distribution of contact types for compound **1** is smoother than that for **NAPTO** both statistically and geometrically. This can be interpreted as the manifestation of more isotropic molecular environment in compound **1** which may prevent from some of vibrational relaxation processes occurred upon detonation.

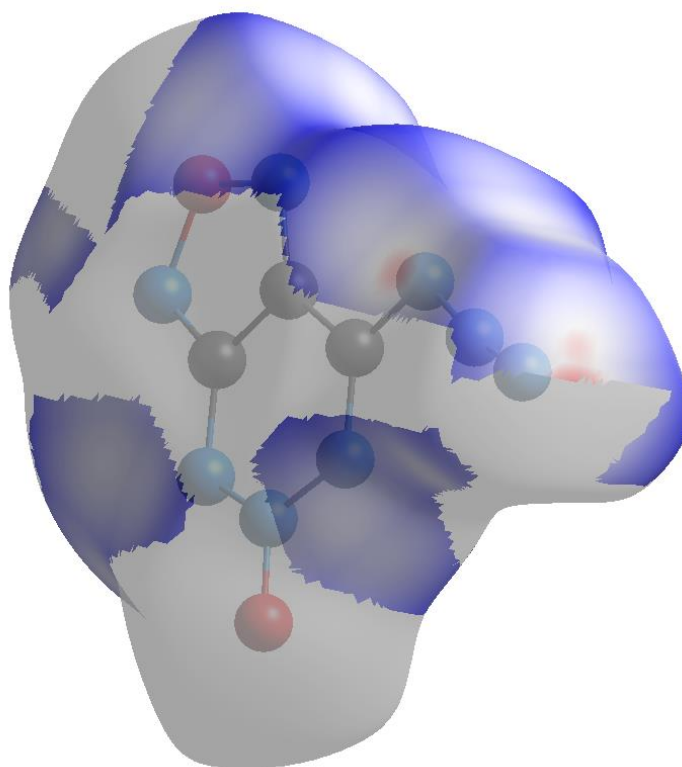
To some extent, the difference in the crystal packing anisotropy of compound **1** and **NAPTO** also follows from the analysis of the pair interaction energies calculated at the CE-B3LYP/6-31G(d,p) level and corresponding energy frameworks.<sup>[S15]</sup> The layer-type packing can be traced for **NAPTO** (Figure S4), although the interactions between layers in turn out to be even slightly stronger than those within them ( $-10.8 \text{ kcal mol}^{-1}$  vs.  $-10.0 \text{ kcal mol}^{-1}$ ). For compound **1**, a sound chain-type packing motif with the parquet-type arrangement of molecules is clearly observed (Figure S5). This, especially taking into account weaker interaction within these chains ( $-8.6 \text{ kcal mol}^{-1}$ ) in comparison to the mentioned interactions in **NAPTO**, once again indicates a more isotropic crystal packing of compound **1**. The difference in crystal lattice energies estimated as a one half of all pair interaction energies (the condition of a molecule to form contacts shorter than  $10 \text{ \AA}$  produced 96 and 80 molecules for compound **1** and **NAPTO**, respectively) also agrees well with the larger sensitivity of compound **1** ( $-25.6$  vs.  $-28.9 \text{ kcal mol}^{-1}$ ).



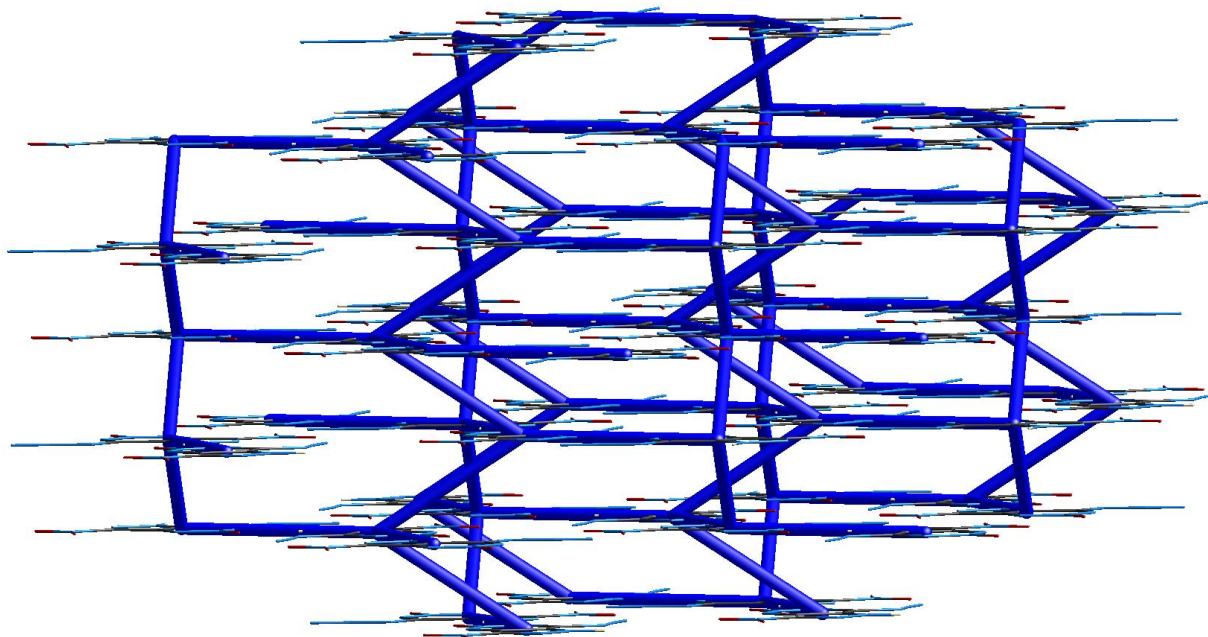
**Figure S1** The Hirshfeld surfaces colored by the  $d_{\text{norm}}$  value for compound **1** (left) and **NAPTO** (right).



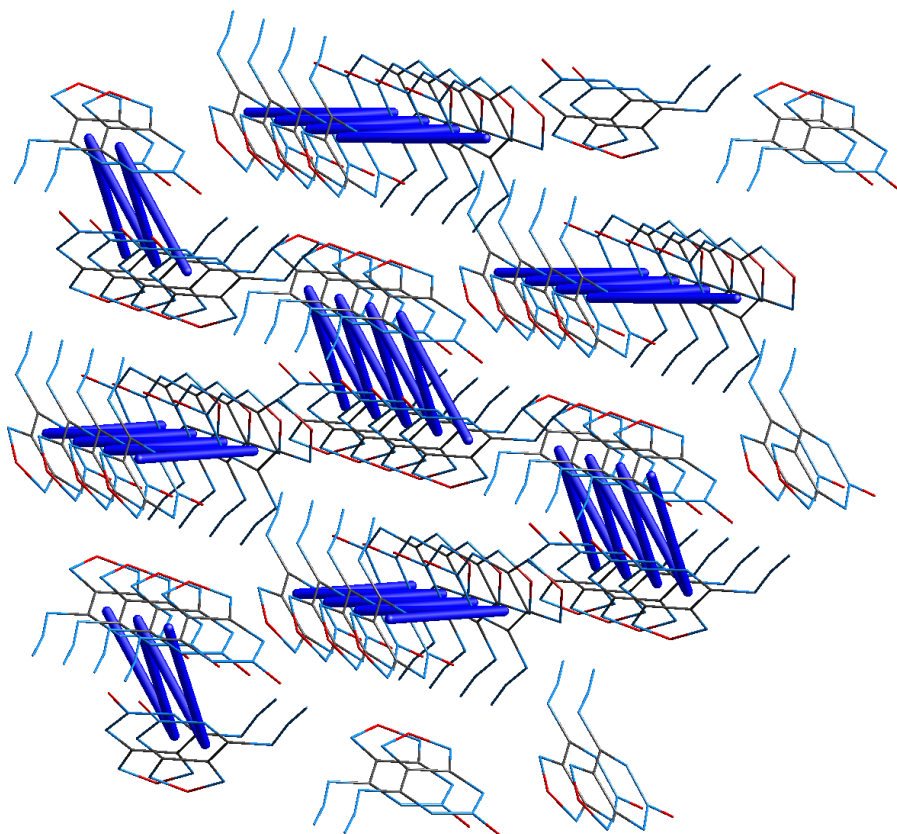
**Figure S2** The distributions of types of close contacts (%) penetrating Hirshfeld surfaces of compound **1** and NAPTO.



**Figure S3** The Hirshfeld surface for compound **1** colored by the  $d_{\text{norm}}$  value for contacts of N...N type.



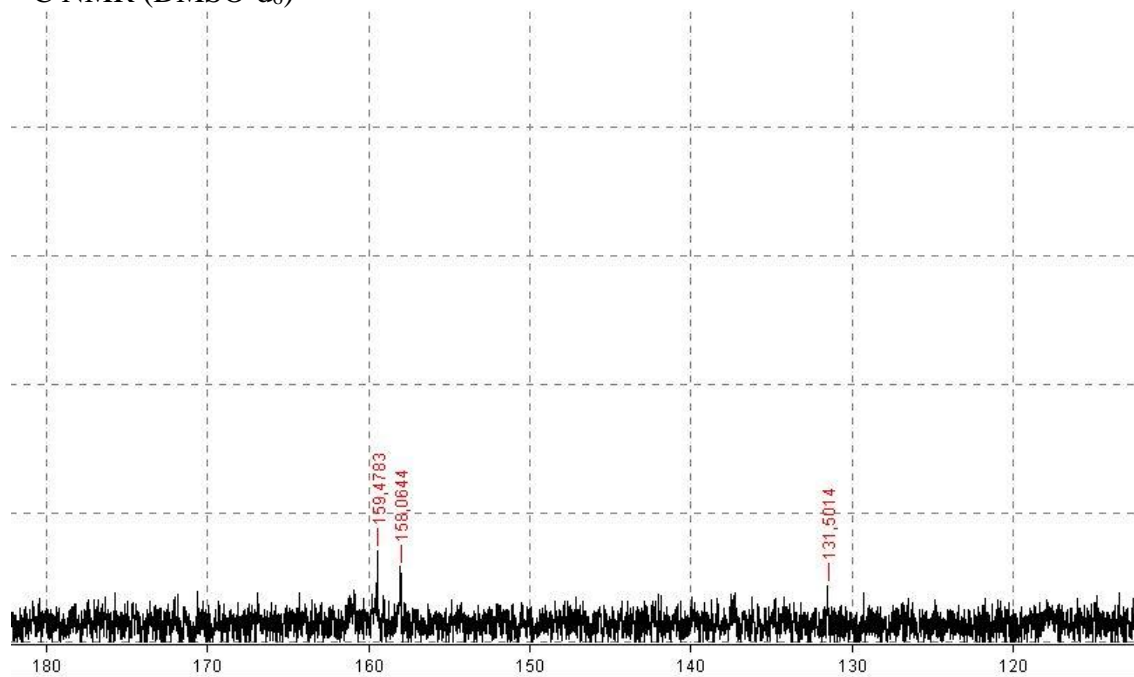
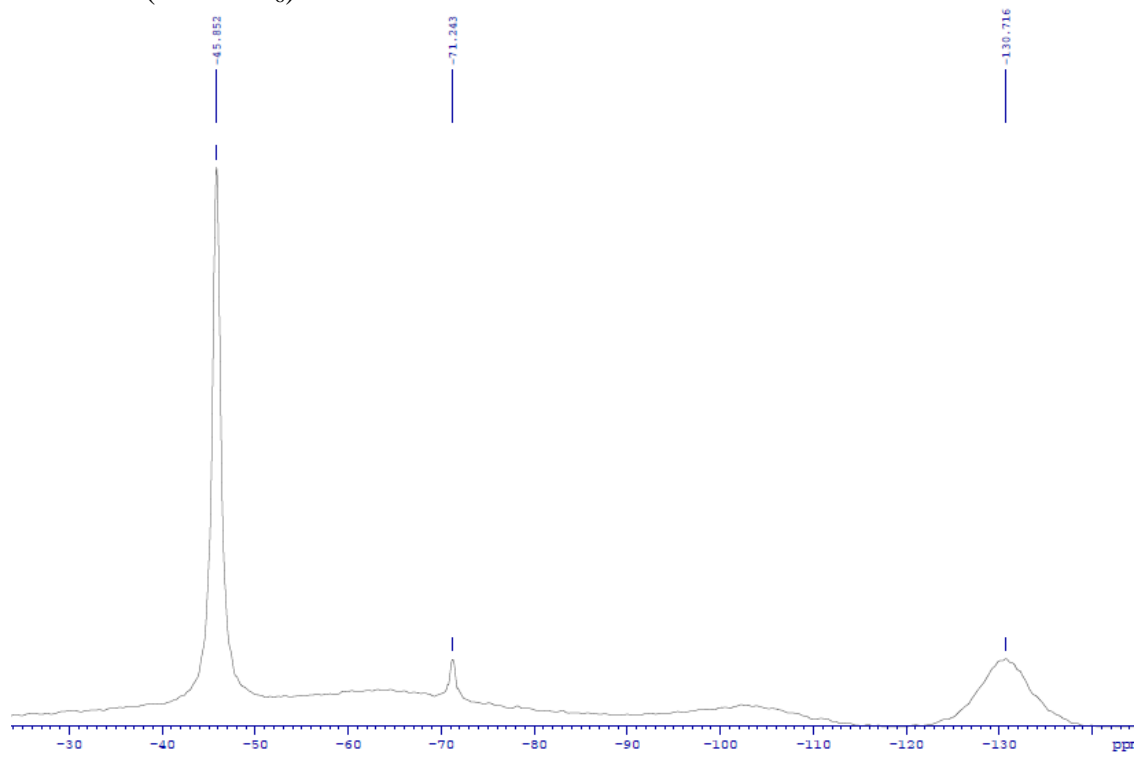
**Figure S4** A fragment of crystal packing of **NAPTO** demonstrating the energy framework calculated at the CE-B3LYP/6-31G(d,p) level (20 kJ mol<sup>-1</sup> as a cut-off).

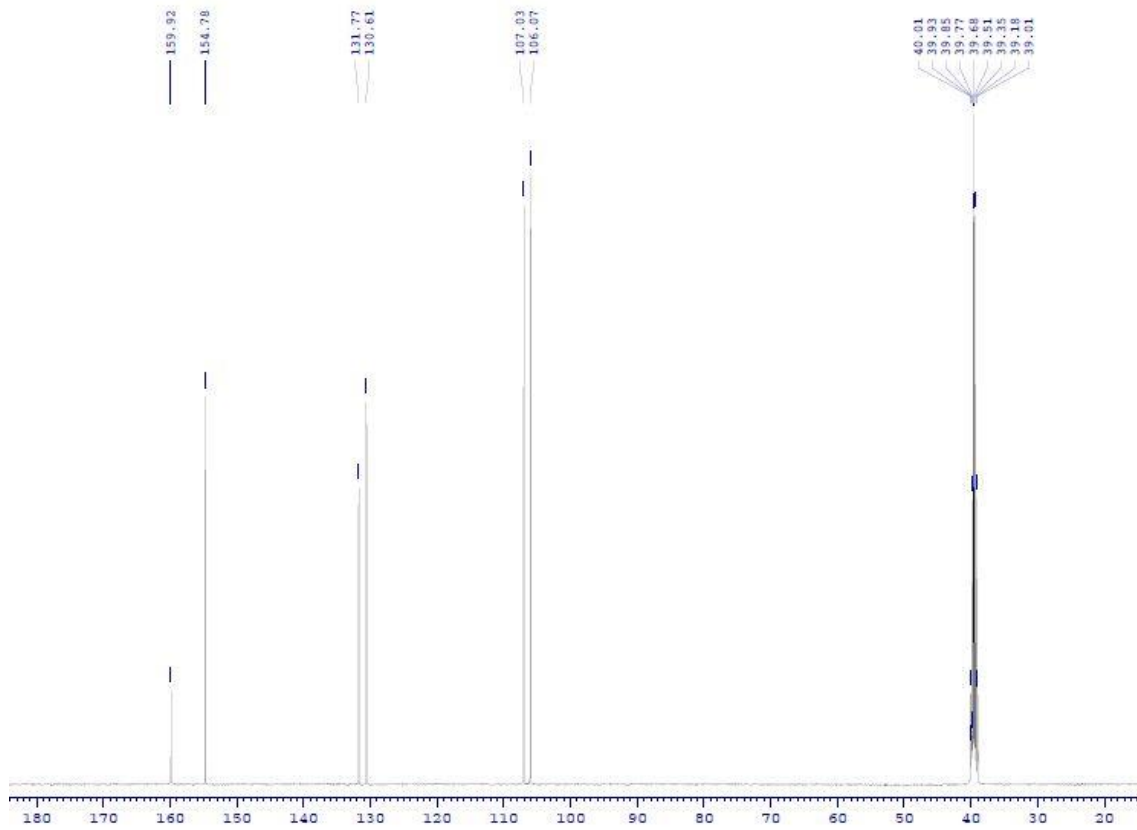


**Figure S5** A fragment of crystal packing of compound **1** demonstrating the energy framework calculated at the CE-B3LYP/6-31G(d,p) level (20 kJ mol<sup>-1</sup> as a cut-off).

## References

- S1. V. G. Andrianov and A. V. Ereemeev, *Chem. Heterocycl. Compd.*, 1994, **30**, 608 (*Khim. Geterotsikl. Soedin.*, 1994, **30**, 693).
- S2. A. I. Stepanov, V. S. Sannikov, D. V. Dashko, A. G. Roslyakov, A. A. Astrat'ev and E. V. Stepanova, *Chem. Heterocycl. Compd.*, 2015, **51**, 350.
- S3. V. G. Andrianov, V. G. Semenikhina and A. V. Ereemeev, *Chem. Heterocycl. Compd.*, 1992, **28**, 581 (*Khim. Geterotsikl. Soedin.*, 1992, **28**, 687).
- S4. A. I. Stepanov, V. S. Sannikov, D. V. Dashko, A. G. Roslyakov, A. A. Astrat'ev and E. V. Stepanova, *Chem. Heterocycl. Compd.*, 2017, **53**, 746.
- S5. V. P. Zelenov, S. S. Bukalov, L. A. Leites, I. S. Bushmarinov, M. I. Struchkova, A. O. Dmitrienko and V. A. Tartakovsky, *ChemistrySelect*, 2017, **2**, 11886.
- S6. V. P. Zelenov, D. V. Khakimov, I. V. Fedyanin and I. A. Troyan, *J. Raman Spectrosc.*, 2019, **50**, 1753.
- S7. V. P. Zelenov, V. A. Tartakovsky and S. S. Bukalov, *Patent RU 2558115 C1*, 2015.
- S8. M. J. Frisch, G. W. Trucks, H. B. Schlegel, G. E. Scuseria, M. A. Robb, J. R. Cheeseman, J. A. Montgomery, Jr., K. N. Kudin, J. C. Burant, J. M. Millam, S. S. Iyengar, J. Tomasi, V. Barone, B. Mennucci, M. Cossi, G. Scalmani, N. Rega, G. A. Petersson, H. Nakatsuji, M. Hada, M. Ehara, K. Toyota, R. Fukuda, J. Hasegawa, M. Ishida, T. Nakajima, Y. Honda, O. Kitao, H. Nakai, M. Klene, X. Li, J. E. Knox, H. P. Hratchian, J. B. Cross, V. Bakken, C. Adamo, J. Jaramillo, R. Gomperts, R. E. Stratmann, O. Yazyev, A. J. Austin, R. Cammi, C. Pomelli, J. W. Ochterski, P. Y. Ayala, K. Morokuma, G. A. Voth, P. Salvador, J. J. Dannenberg, V. G. Zakrzewski, S. Dapprich, A. D. Daniels, M. C. Strain, O. Farkas, D. K. Malick, A. D. Rabuck, K. Raghavachari, J. B. Foresman, J. V. Ortiz, Q. Cui, A. G. Baboul, S. Clifford, J. Cioslowski, B. Stefanov, G. Liu, A. Liashenko, P. Piskorz, I. Komaromi, R. L. Martin, D. J. Fox, T. Keith, M. A. Al-Laham, C. Y. Peng, A. Nanayakkara, M. Challacombe, P. M. W. Gill, B. Johnson, W. Chen, M. W. Wong, C. Gonzalez and J. A. Pople, *Gaussian 03, Revision E.01*, Gaussian, Wallingford, CT, 2004.
- S9. M. S. Westwell, M. S. Searle, D. L. Wales and D. H. Williams, *J. Am. Chem. Soc.*, 1995, **117**, 5013.
- S10. G. M. Sheldrick, *Acta Crystallogr.*, 2015, **C71**, 3.
- S11. Y. Feng, M. Deng, S. Song, S. Chen, Q. Zhang and J. M. Shreeve, *Engineering*, 2020, **6**, 1006.
- S12. P. R. Spackman, M. J. Turner, J. J. McKinnon, S. K. Wolff, D. J. Grimwood, D. Jayatilaka and M. A. Spackman, *J. Appl. Crystallogr.*, 2021 **54**, 1006.
- S13. M. A. Spackman and D. Jayatilaka, *CrystEngComm*, 2009, **11**, 19.
- S14. Y. Ma, A. Zhang, X. Xue, D. Jiang, Y. Zhu and C. Zhang, *Cryst. Growth Des.*, 2014, **14**, 6101.
- S15. C. Mackenzie, P. R. Spackman, D. Jayatilaka and M. A. Spackman, *IUCrJ*, 2017, **4**, 575.

Spectra of compound **1** $^{13}\text{C}$  NMR (DMSO- $d_6$ ) $^{14}\text{N}$  NMR (DMSO- $d_6$ )

Spectra of compound **5** $^{13}\text{C}$  NMR (DMSO- $d_6$ ) $^{14}\text{N}$  NMR (DMSO- $d_6$ )